New Cosmological Data and the Values of the Fundamental Parameters
IAU Symposium, Vol. 201, 2005
Anthony Lasenby and Althea Wilkinson, eds.

The Sunyaev-Zel'dovich Effect and Cosmological Parameters

Mark Birkinshaw
Department of Physics, University of Bristol, Tyndall Avenue, Bristol BS8 1TL, UK

Abstract. Improved Sunyaev-Zel'dovich effect data from interferometers and single dishes, and new X-ray data from Chandra and XMM, are allowing a more detailed examination of the Sunyaev-Zel'dovich effect/X-ray technique for the measurement of distance, and hence the Hubble constant. This article reviews progress so far and the current results for H_0, and discusses the potential of surveys for the Sunyaev-Zel'dovich effect as tests for cosmological parameters and cluster evolution.

1. Introduction: the Sunyaev-Zel'dovich effect

The Sunyaev-Zel'dovich effect (SZE) originates in the inverse-Compton scattering of the cosmic microwave background radiation by hot gas, especially gas in the atmospheres of clusters of galaxies (Sunyaev & Zel'dovich 1972). The physics of the effect have been reviewed recently by Rephaeli (1996) and Birkinshaw (1999), and can usefully be discussed in two parts.

1.1. The thermal SZE

The dominant effect is proportional to the average fractional frequency change of a scattered photon, $\Delta\nu/\nu \propto k_{\rm B}T_{\rm e}/m_{\rm e}c^2$, and to the optical depth to electron scattering, $\tau_{\rm e}$. Since both quantities are of order 10^{-2} for an X-ray bright cluster of galaxies, the largest brightness change in the microwave background radiation that might be expected is a decrease of about 1 mK. For a cluster with an angular size of 1 arcmin, the corresponding flux density is about -0.1 mJy at 30 GHz.

Rephaeli (1995) and others have perfomed a detailed calculation of the spectrum of the thermal SZE, taking account of relativistic effects, which are important because a significant fraction of the electrons in a cluster with $k_{\rm B}T_{\rm e} \approx 10$ keV have velocities $> 0.2c$. For high frequencies and the hottest clusters the spectrum is a complicated function of frequency and electron temperature. For low frequencies ($\lesssim 90$ GHz) and cluster temperatures ($\lesssim 10$ keV) the spectrum has a form independent of cluster properties (Fig. 1). In either case the amplitude of the effect at zero frequency is

$$\Delta T_{\rm T0} = 2\,T_{\rm rad}\,y_{\rm e} = 2\,T_{\rm rad}\int n_{\rm e}\,\sigma_{\rm T}\,\frac{k_{\rm B}\,T_{\rm e}}{m_{\rm e}\,c^2}\,dl \qquad (1)$$

where $n_{\rm e}$ and $T_{\rm e}$ are the electron number density and temperature, the integral is along the line of sight, $T_{\rm rad}$ is the radiation temperature of the microwave

https://doi.org/10.1017/S0074180900216380 Published online by Cambridge University Press

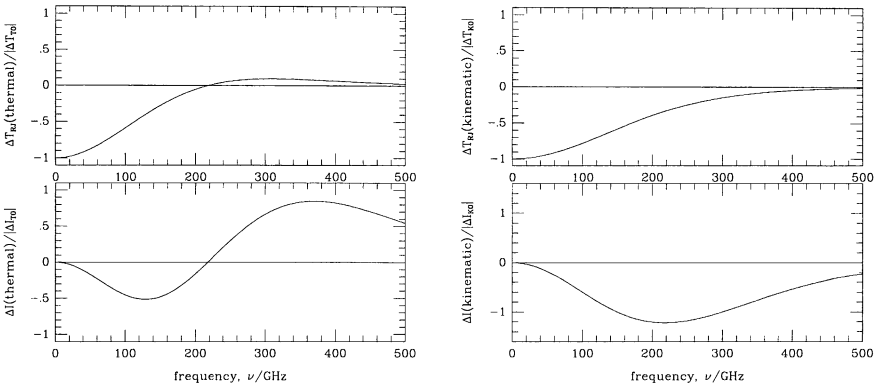

Figure 1. Frequency-dependence of the thermal (left) and kinematic (right) SZEs expressed in terms of brightness temperature (upper plots) and intensity (lower plots), in the non-relativistic limit.

background, and c, $k_{\rm B}$, $\sigma_{\rm T}$ and $m_{\rm e}$ are the speed of light, the Boltzmann constant, the Thomson scattering cross-section, and the electron mass. $y_{\rm e}$ is the Comptonization parameter, and is proportional to the line-of-sight integrated electron pressure. $\Delta T_{\rm T0}$ is independent of redshift.

Non-thermal electrons, such as those in radio galaxies or cluster radio halo sources, also have an effect on the microwave background radiation. The amplitude of this non-thermal SZE is proportional to $\tau_{\rm e}$, rather than $y_{\rm e}$. However relativistic electrons have significant $\tau_{\rm e}$ and produce a detectable SZE only if the energy spectrum of the synchrotron-emitting electrons extends to unexpectedly low energies (Birkinshaw 1999).

1.2. Kinematic effect

A moving scattering medium produces a change in the brightness of radiation passing through it. The brightness temperature change has the same spectral form as primordial fluctuations in the background radiation (Fig. 1). The amplitude of the brightness temperature change at zero frequency is

$$\Delta T_{\rm K0} = \frac{v_{\rm z}}{c}\,\tau_{\rm e}\,T_{\rm rad} \tag{2}$$

where $v_{\rm z}$ is the peculiar velocity of the scattering medium along the line of sight away from the observer. This effect is smaller than the thermal SZE by a factor

$$\frac{\Delta T_{\rm K0}}{\Delta T_{T0}} \approx 0.085\left(v_{\rm z}/1000\ {\rm km\,s^{-1}}\right)\left(k_{\rm B}T_{\rm e}/10\ {\rm keV}\right)^{-1} \tag{3}$$

but has the same angular structure if the cluster is isothermal. It is therefore hard to detect in the presence of the larger thermal effect: separation of the two signals relies on their different spectra (Fig. 1), with the kinematic effect dominating near the frequency at which the thermal effect changes sign

$$\nu_{\rm zero} = (217.7 \pm 0.2) \times \left(1 + 0.022\,(k_{\rm B}T_{\rm e}/10\ {\rm keV})\right)\quad {\rm GHz}. \tag{4}$$

https://doi.org/10.1017/S0074180900216380 Published online by Cambridge University Press

Even at $\nu_{\rm zero}$ the kinematic SZE will be difficult to detect unambiguously, because of confusion from primordial fluctuations in the microwave background.

$\Delta T_{\rm K0}$, like $\Delta T_{\rm T0}$, is redshift independent. Practical observations always cause $\Delta T_{\rm K0}$ and $\Delta T_{\rm T0}$ to be averaged over some solid angle, and this introduces a redshift dependence into the observed brightness temperature changes.

1.3. Other cluster-induced effects

Clusters induce other secondary fluctuations in the microwave background radiation, including polarization associated with the thermal and kinematic SZEs (but weaker by factors $\sim \frac{v_z}{c}$ or $\tau_{\rm e}$; e.g., Itoh et al. 1999; Challinor et al. 1999), and intensity effects from the time-varying gravitational field experienced by a photon passing through a non-static cluster.

This latter effect may arise because the cluster is contracting (Rees & Sciama 1968), or moving across the line of sight (e.g., Pyne & Birkinshaw 1993). The fractional brightness change caused in the microwave background is of order $\frac{\Phi}{c^2}\frac{v}{c}$, where Φ is the gravitational potential, and v is the speed of the change in structure. While these effects would provide exciting information, they are undetectably small and confused with primordial fluctuations.

2. Observations of the Sunyaev-Zel'dovich effects

The SZEs are relatively easily detected provided that the observing technique is able to separate them from contaminating astrophysical or terrestrial signals. The major issue for many clusters is of distinguishing the SZEs in the presence of non-thermal and often variable radio sources. Extended radio emission from cluster radio halo sources may also be a problem, but the steep radio spectra of such sources usually means that their contribution is small.

The background of primordial structure in the microwave background radiation is also a confusing signal. The strongest thermal effects overwhelm the primordial signal, but smaller, lower-temperature, clusters have effects < 0.1 mK, and these may be confused by primordial fluctuations. In this case, multiple frequency bands must be observed, and spectral separation attempted.

Single-dish measurements of the microwave background anisotropies towards clusters of galaxies are now relatively routine. This technique was used for the first detections of clusters (Birkinshaw, Gull & Northover 1978). While it is particularly well suited to the measurement of the integrated SZE signal, such observations suffer from systematic errors to do with imperfect subtraction of radio sources near the line of sight, atmospheric noise, and spillover, so particularly careful beam-switched and position-switched measurements are needed. Nevertheless, this remains one of the fastest methods of surveying a sample of clusters (e.g., Myers 2000).

Many difficulties with systematic errors are avoided by observing with an interferometer, although care has to be taken that the shortest baselines adequately sample the Fourier components that contain most of the SZE signal. Well-designed configurations have many short baselines for detecting the SZE, and a similar number of longer baselines which resolve out the cluster but provide contemporaneous measurements of small-scale contaminating radio sources, so that they can be subtracted accurately. A major advantage of interferometers

https://doi.org/10.1017/S0074180900216380 Published online by Cambridge University Press

is that they produce an image of the cluster, although the raw visibilities are more useful for model fitting. The first interferometric detection of a cluster (Jones et al. 1993) has now been followed by extensive mapping campaigns, for example Carlstrom et al. (1996, 2000); Saunders et al. (2000).

Bolometric observations of clusters, using arrays on mm-wave telescopes, also produce good results, although they have to contend with difficult atmospheric conditions. These observations are performed at high frequency (> 100 GHz), and so must be interpreted using the relativistic form of the spectrum, but by using multiple bands are able to separate the thermal SZE from the kinematic effect or primordial fluctuations (Holzapfel et al. 1997).

3. Hubble diagram

A major reason for the interest in the thermal SZE is that it can be used to measure the Hubble constant. The method relies on the different dependences on cluster properties and distance of the thermal SZE and the X-ray surface brightness of a cluster. The quantity $\Delta T_{\rm T0} \propto n_{\rm e0}\, T_{\rm e0}\, r_{\rm c}$ (Eq. 1), where $n_{\rm e0}$, $T_{\rm e0}$, and $r_{\rm c}$ are the central electron density, central temperature, and core radius of the cluster. Similarly, the central X-ray surface brightness, $\Sigma_{\rm X0} \propto n_{\rm e0}^2\, \Lambda(T_{\rm e0})\, r_{\rm c}$ where $\Lambda(T_{\rm e})$ is the emissivity of the gas as a function of temperature. If the temperature of the gas is known from X-ray spectroscopy, then the combination

$$\Lambda(T_{\rm e0})\, T_{\rm e0}^{-2}\, \frac{\Delta T_{\rm T0}^2}{\Sigma_{\rm X0}} \propto r_{\rm c} \quad , \tag{5}$$

and so the core radius can be inferred from observable quantities. When compared with the angular size of the cluster, $\theta_{\rm c}$, the angular diameter distance $d_{\rm A} = r_{\rm c}/\theta_{\rm c}$ can be used to measure the Hubble constant (and other cosmological parameters, if $d_{\rm A}$ can be measured to $z \approx 1$). This technique applies to each cluster as an individual, with the parameters that best describe the cluster's X-ray structure also yielding the constant of proportionality in Eq. (5). The method is *absolute*, and can be applied directly at large redshift, without the need for a cosmic distance ladder. A calculation for Abell 2218 is shown in Fig. 2 (left): note the strong dependence of the estimate of H_0 on the values of the parameters β and $\theta_{\rm c}$ which describe the atmosphere.

A recent compilation of distance estimates made in this way is given in Birkinshaw (1999), and a representative nine-cluster Hubble diagram is shown in Fig. 2 (right). Although a formal analysis of this diagram implies a Hubble constant $H_0 = 55 \pm 10\ {\rm km\,s^{-1}\,Mpc^{-1}}$, this ignores several important issues. First, the result for H_0 depends critically on the absolute flux density calibrations of the radio and X-ray telescopes, and few independent telescopes are involved in Fig. 2. Likely systematic errors of 5 per cent in each scale would lead to a systematic error $\pm 8\ {\rm km\,s^{-1}\,Mpc^{-1}}$ in the result for H_0. Excellent absolute calibrations are essential for the method to be effective.

Second, the method relies on a good model for the structure of the cluster atmosphere. The amplitudes of the central (or other fiducial) SZE and X-ray brightnesses are found and then used to calculate H_0. These amplitudes are obtained by fitting a model structure for the cluster, which may depend on several parameters (β and $\theta_{\rm c}$ in Fig. 2). The resulting model provides the constant of

https://doi.org/10.1017/S0074180900216380 Published online by Cambridge University Press

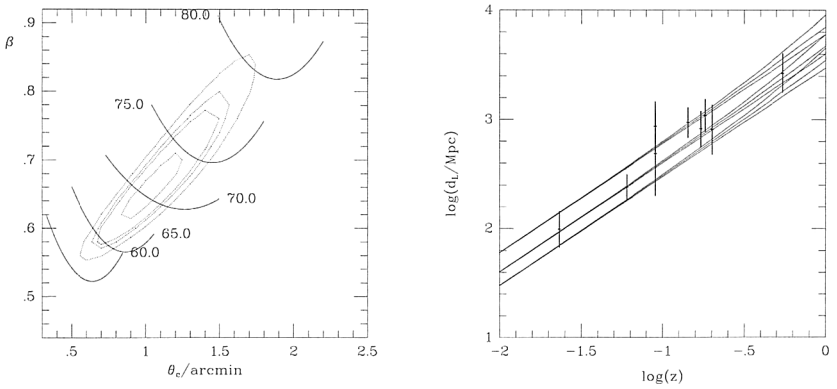

Figure 2. Left, a Hubble constant calculation for Abell 2218 showing χ^2 contours for fits to the X-ray image (dotted contours corresponding to 50, 90, 95 and 99 per cent confidence levels). Solid contours show the value of H_0 as a function of (β, θ_c). Right, a Hubble diagram based on the distances of nine clusters of galaxies as measured by comparing their SZEs and X-ray surface brightnesses. The curves show the luminosity distance as a function of redshift for $H_0 = 50$, 75, and 100 $\mathrm{km\,s^{-1}\,Mpc^{-1}}$ and $q_0 = 0$, $\frac{1}{2}$, and 1.

proportionality in Eq. (5). But the model choice is non-unique, and different choices, like different fit parameters, lead to different results for H_0.

Particular difficulties arise because the X-ray flux of a cluster is more dominated by its central regions than is the thermal SZE. The structure model must be uniformly good at fitting the regions where the fiducial X-ray and SZE amplitudes are found. For single-dish measurements, this may require the model to make a high-quality description of the cluster structure from r_c to $10r_c$. Interferometric data have an advantage here, since they are relatively insensitive to the outer structure of the SZE, and require less model fidelity.

The deprojection implied by model fitting will certainly be wrong if the cluster is non-spherical. Non-spherical clusters increase the noise on the Hubble diagram: if a cluster is extended along the line of sight, then its apparent angular size will be an underestimate of r_c/d_A, and so it will be assigned too large a distance and too small a Hubble constant. This effect leads to biases if clusters are selected for observation based on their X-ray or SZE brightnesses, or even optical richness, because such selections prefer objects extended along the line of sight. This is an important reason for selecting an orientation-independent sample of objects by their *total* X-ray fluxes. For similar reasons, upper limits on ΔT_{T0}, as well as measurements, should be included in Fig. 2.

Unmodelled structures in the cluster atmosphere, such as clumping or thermal gradients, can lead to significant errors for individual clusters, or to systematic errors in the Hubble diagram as a whole. Thus, for example, no sample of clusters can remove the effects of clumping, which cause a one-sided error in the Hubble constant, because clumping always causes the X-ray intensity to be increased relative to the expectations for an unclumped atmosphere.

The number of distance measurements made using this technique is increasing rapidly, with several programmes of parallel X-ray and microwave back-

https://doi.org/10.1017/S0074180900216380 Published online by Cambridge University Press

ground studies of clusters in progress. New measurements, suggesting systematically larger values of H_0 than those appearing in Fig. 2, have recently been presented (e.g., Myers 2000), and approximately double the number of measurements suitable for the determination of H_0.

4. Cluster velocities

The kinematic effect can measure the peculiar radial velocity, v_z, of a cluster only if good spectral separation from the thermal effect is possible. However, an irreducible noise on v_z arises from underlying primordial fluctuations with an identical spectrum (Fig. 1). On angular scales of about 2 arcmin, the primordial signal is expected to be about 10 μK. Eq. (2) shows that this corresponds to a velocity noise $\sim 100\ \mathrm{km\,s^{-1}}$ if the cluster has central scattering optical depth $\tau_{e0} \sim 10^{-2}$. Thus individual rich clusters at $z \gtrsim 0.2$ could be detected (at the 3σ level) in the kinematic effect if their velocities exceed $300\ \mathrm{km\,s^{-1}}$. In practice this measurement is very difficult, and errors of about $\pm 700\ \mathrm{km\,s^{-1}}$ in v_z are the best that have so far been achieved (Holzapfel et al. 1997).

If this technique could be applied to a large sample of clusters, then some statistical measure of the distribution function of peculiar radial velocities, $f(v_z)$, could be made. Such a measurement of the noisiness of the peculiar velocity field on the largest mass scales would be of considerable interest for studies of large-scale structure. The distance-independence of ΔT_{K0} would allow the evolution of $f(v_z)$ to be followed to the earliest redshift at which clusters develop atmospheres with sufficient optical depth. However, if $f(v_z)$ is only $\sim 100\ \mathrm{km\,s^{-1}}$ wide, ΔT_{K0} would have to be measured for about 30 clusters to ± 10 μK for useful results.

While such a study is not out of the question, it would be subject to systematic errors in v_z arising from thermal substructure within the cluster, since simultaneous understanding of the kinematic and thermal effects is necessary to measure the τ_e factor in Eq. (2). At the level of $100\ \mathrm{km\,s^{-1}}$, internal gas flows within the cluster — large-scale flows connected with accretion events or cooling, and small-scale flows associated with galaxies — may make it difficult to extract the cluster peculiar velocity even from excellent measurements of ΔT_{K0}.

5. Cluster baryon fraction

The thermal SZE provides a more direct measure of the total gas content of a cluster than an X-ray flux, since ΔT_{T0} is proportional to n_e. Thus for an isothermal cluster, the total SZE flux density is proportional to the total electron count in the cluster atmosphere. Since the atmospheres of rich clusters of galaxies contain more mass than the member galaxies, a thermal SZE flux density can be converted into a good estimate of the baryonic mass of a cluster if T_e is known from an X-ray spectrum.

A comparison of this mass with the total mass obtained by gravitational shear mapping yields a clean measurement of the baryonic mass fraction of a cluster. Indeed, this comparison can be made at image level: an SZE image is a measure of the baryonic column densities across the face of a cluster, while a

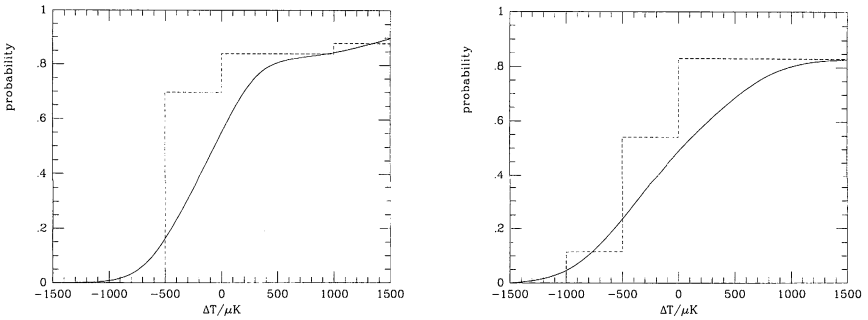

Figure 3. The distributions of brightness temperature differences for the NEP sample (left) and XBACs sample (right), as measured with the OVRO 40-m telescope. The solid lines show the apparent cumulative distributions, and the dotted lines the underlying cumulative distributions expressed as a histogram.

gravitional shear map is a measure of total column densities. The ratio provides a map of the baryonic mass fraction in a cluster.

In the absence of a gravitational shear map, X-ray data can be used to calculate a mass for a cluster under the usual assumption that the cluster atmosphere is in hydrostatic equilibrium. This can already be done for every cluster being used for Hubble diagram work. The current result for the baryonic mass fraction shows considerable scatter, but appears to be $(0.07 \pm 0.02)\, h_{100}^{-1}$ at all redshifts (Myers et al. 1997; Grego et al. 2000).

In the future this work could measure the baryonic mass as a function of radius within a cluster, and test whether clusters constitute a fair sample of the mass content of the Universe. Alternatively, it can be used to estimate the contribution of matter to Ω_0 (Grego et al. 2000).

6. Surveys and samples

All sensitive observations of the SZEs to date have been targetted at selected clusters. Blind surveys for the thermal SZE are now feasible using improved ground-based array receivers and bolometers, although considerable time is required to cover a useful sky area ($10 - 100$ deg^2). Balloon-borne telescopes are reaching the sensitivities and angular resolutions needed, and the MAP and Planck satellites will certainly have good sensitivity: Planck is likely to detect $\gtrsim 10^4$ thermal SZEs (e.g., da Silva et al. 2000), and to make a statistical measure of the kinematic effect.

Current SZE work is usually restricted to the hottest and most X-ray luminous clusters because of the expected correlation between $\Delta T_{\rm T0}$ and X-ray luminosity. This strategy may lead to misinterpretation of the detections, for example if they are used to estimate the value of the Hubble constant, and the intrinsic structural properties of clusters correlate with X-ray luminosity.

With this in mind, I have conducted surveys of 26 Abell clusters in the North Ecliptic Pole (NEP) region, and 12 Abell clusters which appear in the sample of

https://doi.org/10.1017/S0074180900216380 Published online by Cambridge University Press

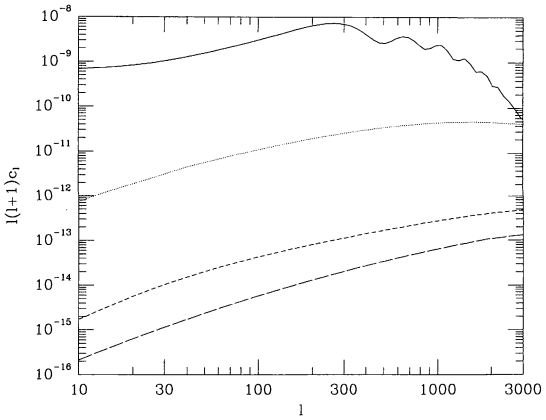

Figure 4. The power spectrum of primordial fluctuations in the microwave background radiation (upper line), the thermal SZE (dotted line), the kinematic SZE (dashed line), and the Rees-Sciama effect from moving clusters (long dashed line) for a ΛCDM cosmology.

X-ray Brightest Abell Clusters (XBACs; Ebeling et al. 1996). Although these surveys are not blind, nor selected in an orientation-independent fashion, the optical selection does differ from the anecdotal selections that have characterised much of the SZE work to date. No attempt was made to select clusters without radio sources. The surveys were conducted with the 40-m OVRO telescope, and a representation of the results is shown in Fig. 3.

Significant SZEs were detected from 8 clusters in the combined sample. A statistical analysis indicates that 40 per cent of all clusters of the type sampled show SZEs exceeding 100 μK, but that about 10 per cent are contaminated by bright radio sources (more than 1000 μK at 18 GHz). As might be expected, XBACs tend to show larger SZEs and stronger radio sources than NEP clusters.

These results suggest that a larger targetted or blind survey is likely to be successful. A survey to a depth of ~ 30 μK should detect about 40 per cent of all rich clusters, even without simultaneous subtraction of contaminating radio sources.

7. Contributions to the power spectrum

Since clusters of galaxies can produce large microwave background structures in the form of the thermal and kinematic SZEs, and smaller effects of Rees-Sciama type, it is of interest to calculate their contribution to the power spectrum of brightness fluctuations. A representative simulation is shown in Fig. 4. It can be seen that cluster thermal SZEs make a small (< 1 per cent) contribution to the power spectrum on large angular scales ($l \lesssim 500$), but become important on scales $l \gtrsim 3000$ (corresponding to angular scales of a few arcmin). The kinematic SZE effect is never important, and neither is the Rees-Sciama effect (Molnar & Birkinshaw 2000).

https://doi.org/10.1017/S0074180900216380 Published online by Cambridge University Press

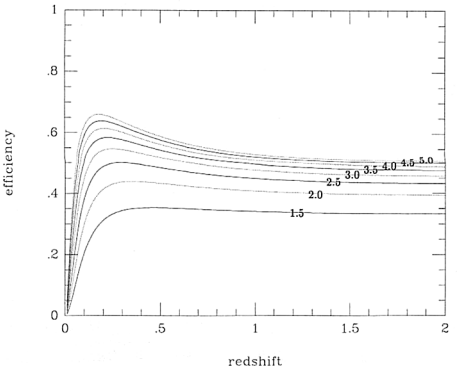

Figure 5. The efficiency of OCRA observations of clusters of galaxies as a function of redshift and beam separation. With 2.5 arcmin beam separation and 1 arcmin beams, OCRA will be sensitive to cluster thermal SZEs at $z > 2$.

The relative powers in primordial fluctuations and the thermal SZE are a strong function of cosmology, depending particularly on the redshifts at which clusters acquire significant atmospheres, and the run of angular diameter distance with redshift. Measurements of the shape and amplitude of the power spectrum in the thermal SZE at $l \gtrsim 1000$ will lead to strong constraints on models of cluster formation and evolution. This type of data will be provided by large-area blind surveys.

8. Future work

MAP and Planck, with their high sensitivities and all-sky surveys, will produce new SZE-selected samples of clusters. However, of necessity these missions have only modest angular resolution at the frequencies where the thermal SZE is large, and so the resulting sample will show selection effects from beam dilution.

Ground-based telescopes, tailored for SZE measurements, will dominate the study of cluster evolution because of their potential to detect clusters on small angular scales. Interferometers with baselines in the 100λ to 5000λ range and operating wavelengths $\lambda = 0.2 - 1$ cm are expected to be particularly important, since they will be capable of high sensitivity and tuned angular resolution. They are therefore suitable for extremely deep survey work, and high-quality mapping of selected clusters. The AMiBA project (Lo et al. 2000) falls into this category.

The fastest surveys, however, are likely to be made with cm-wave receiver arrays (such as OCRA; Browne et al. 2000) or mm-wave bolometer arrays (such as Bolocam; Glenn et al. 1998). It is now possible to make arrays of hundreds of receiver or bolometer elements which, mounted on a large telescope, achieve arcminute resolution and can survey to sensitivity ~ 20 μK at a rate ~ 1 deg^2 per day. Arrays such as OCRA will be capable of detecting clusters at redshifts $z > 2$ with high efficiency (Fig. 5) and will provide the definitive counts of SZE clusters that can set strong constraints on models of large scale structure formation.

https://doi.org/10.1017/S0074180900216380 Published online by Cambridge University Press

Within the next decade we will have samples of $> 10^4$ clusters selected by SZE surveys. For some hundreds of these we should have high-quality interferometric maps suitable for detailed comparison with gravitational shear maps and sensitive X-ray images with spatially resolved spectroscopy. These comparisons will yield information on the baryonic mass fraction in clusters, and its evolution with redshift, as well as Hubble diagrams populated with large numbers of clusters to $z \approx 1$. Further information on the development of large-scale structure should come from statistical measures of cluster peculiar velocities.

While results from the SZE are already impressive, we have barely started making use of this important cosmological tool.

References

Birkinshaw, M., Gull, S. F., & Northover, K. J. E. 1978. Nature, 275, 40
Birkinshaw, M., Gull, S. F., & Hardebeck, H. E. 1984. Nature, 309, 34
Birkinshaw, M. 1999. Phys. Reports, 310, 97
Browne, I. W. A. et al. 2000. Proc. SPIE, in press
Carlstrom, J. E., Joy, M., & Grego, L. 1996. ApJ, 456, L75 and erratum 461, L59
Carlstrom, J. E. et al. 2000. Physica Scripta, T85, 148
Challinor, R., Ford, M., & Lasenby, A. N., 1999. MNRAS, 312, 159
da Silva, A. C., Domingos, B., Liddle, A. R., & Thomas, P. A. 2000. MNRAS, 317, 37
Ebeling, H. et al. 1996. MNRAS, 281, 799 and erratum 283, 1103
Glenn, J. et al. 1998. Proc. SPIE, 3357, 326
Grego, L. et al. 2000. ApJ, submitted
Holzapfel, W. L. et al. 1997. ApJ, 481, 35
Itoh, N., Nozawa, S., & Kohyama, Y., 1999. ApJ, 533, 588
Jones, M. et al. 1993. Nature, 365, 320
Kompaneets, A. S. 1956. Zh. Eksp. Fiz. Teor., 31, 876
Lo, K. Y. et al. 2000. These proceedings
Molnar, S. M. & Birkinshaw, M. 2000. ApJ, 537, 542
Myers, S. T. et al. 1997. ApJ, 485, 1
Myers, S. T. 2000. These proceedings
Pyne, T. & Birkinshaw, M. 1993. ApJ, 415, 459
Rees, M. J. & Sciama, D. W. 1968. Nature, 217, 511
Rephaeli, Y. 1995. ApJ, 445, 33
Rephaeli, Y. 1996. ARA&A, 33, 541
Saunders, R. et al. 2000. MNRAS, in press
Sunyaev, R. A. & Zel'dovich, Ya.B. 1972. Comm. Ap. Sp. Phys., 4, 173